

## The current-voltage characteristics of a large probe in low Earth orbit: TSS-1R results

D.C. Thompson<sup>1</sup>, C. Bonifazi<sup>2</sup>, B.E. Gilchrist<sup>3</sup>, S.D. Williams<sup>4</sup>, W.J. Raitt<sup>1</sup>, J.-P. Lebreton<sup>5</sup>, W.J. Burke<sup>6</sup>, N. H. Stone<sup>7</sup>, K. H. Wright, Jr.<sup>8</sup>

**Abstract.** Measurements of the current collected by the Tethered Satellite System (TSS) satellite as a function of voltage and ambient plasma parameters are presented. The satellite current is found to vary approximately with the square root of the potential from below 10 to nearly 1200 V. The collected current exceeded premission expectations, based on the Parker and Murphy [1967] collection model, by factors of two to three. Possible reasons for discrepancies between the measurements and model are briefly discussed.

### Introduction

During the reflight of the joint National Aeronautics and Space Administration (NASA) and Italian Space Agency (ASI) Tethered Satellite System (TSS-1R), a 1.6 m diameter spherical, conducting satellite was deployed from the space shuttle Columbia. The satellite was connected to the Orbiter by an electrically conducting tether, which was insulated from the surrounding ionospheric plasma. A detailed description of the tethered satellite system is given by *Dobrowolny and Stone* [1994]. One of the primary electrodynamic objectives of the TSS-1R mission was to quantify the capability of the ionospheric plasma to carry currents to and from the tether system. The current-carrying capability of the plasma was anticipated to be the factor limiting the ability of the system to generate electrical power and thrust (drag). Further, imposition of the current in the tether system has provided stimulus for laboratory simulation studies of current closure mechanisms across a magnetized plasma [*Stenzel and Urrutia*, 1997].

Of the several measurements in the tether system the most fundamental is the current collected by the satellite as a function of its potential, the ambient plasma density, and

temperature. This is the so called current-voltage (I-V) characteristic. The I-V response of the TSS was determined during its first mission [*Dobrowolny et al.*, 1995] but the voltage range was limited to a few tens of volts owing to the relatively short deployment distance. During TSS-1R, this range was extended to nearly 1200V during controlled charging events reported here, and to as much as 1400V during the tether failure event [*Gilchrist et al.*, 1997].

We have performed a careful empirical analysis of the TSS measurements and report the satellite's I-V characteristics and the range of uncertainty bounding these curves. The currents measured were approximately two to three times larger than premission expectations. Although several possible explanations for this current enhancement are proposed in this issue, controversy remains. This paper is intended to establish a common point of departure for models propounding to explain the TSS-1R I-V characteristics.

### Tether Circuit

The orbital motion of the satellite-tether-Orbiter system created an electromotive force along the tether,  $\phi_{emf} = \mathbf{v} \times \mathbf{B} \cdot \mathbf{L}$ , where  $\mathbf{v}$  is the velocity of the tether in the local plasma frame,  $\mathbf{B}$  is the geomagnetic field, and  $\mathbf{L}$  is the vector from the Orbiter to the satellite. Owing to the prograde orbit and upward deployment, the potential of the satellite was positive with respect to the Orbiter. Current in the tether was controlled by instrumentation on the Orbiter [*Bonifazi et al.*, 1994; *Aguero et al.*, 1994]. Data presented in this paper were obtained during times when the tether current was controlled by the ASI Electron Gun Assembly (EGA) [*Bonifazi et al.*, 1994]. In this configuration, the cathode and anode of the EGA electrically connected to the tether and to the Orbiter ground, respectively. Thus, the tether directly provided both the beam current and accelerating potential. The Orbiter ground was electrically isolated from the TSS circuit and floated at low potentials with respect to the ambient plasma except when beam-generated electrons impacted Orbiter surfaces in large numbers [*Burke et al.*, 1997].

The current collected by the satellite is equal to that flowing in the tether. The tether current was measured directly by two ammeters; on the satellite and the Orbiter ends of the tether. Both instruments operated as expected, producing essentially identical values of calibrated currents.

Several instrument packages were included on the satellite to, among other things, measure the satellite potential relative to the ambient plasma [*Stone et al.*, 1994; *Dobrowolny et al.*, 1994]. Analysis of these data is ongoing, and is only briefly reported here. Instead, the satellite potential,  $\phi_{sat}$  is inferred by requiring that all potentials around the circuit sum to zero. That is,  $\phi_{sat} + \phi_{emf} + I_t R_t + \phi_{to} + \phi_{orb} = 0$ , where  $I_t$  is the measured tether current,  $R_t$  is the tether resistance,  $\phi_{to}$  is the

<sup>1</sup>Center for Atmospheric and Space Science, Utah State University, Logan.

<sup>2</sup>Italian Space Agency, Rome, Italy.

<sup>3</sup>Space Physics Research Laboratory, University of Michigan, Ann Arbor.

<sup>4</sup>Space Telecommunications and Radioscience Lab, Stanford University, Stanford, CA.

<sup>5</sup>Space Science Department, ESA-ESTEC, The Netherlands.

<sup>6</sup>Geophysics Directorate, Phillips Laboratory, Hanscom AFB, MA.

<sup>7</sup>Space Science Laboratory, NASA Marshall Space Flight Center, Huntsville, AL.

<sup>8</sup>Center for Space Plasma and Aeronomic Research, Univ. of Ala. in Huntsville, Huntsville.

measured potential between the tether and the shuttle, and  $\phi_{orb}$  is the Orbiter potential. In this work,  $\phi_{emf}$  is obtained by measuring the open circuit potential between the tether and the Orbiter just prior to tether current events, and correcting its value slightly as a function of time according to the variations of  $\mathbf{v}$ ,  $\mathbf{B}$ , and  $\mathbf{L}$ .  $\phi_{orb}$  is measured by the Shuttle Potential and Return Electron Experiment (SPREE) [Oberhardt *et al.*, 1994]. The first energy step of the SPREE is 10 V, so any Orbiter charging to less than 10 V cannot be determined. The tether resistance,  $R_t$ , was seen to vary significantly depending on deployed length and local day/night, due to the change in resistivity of the copper conductors from variations in tether temperature [Chang *et al.*, 1997]. For the results given here,  $R_t$  is inferred during very low tether current events (less than 10mA) by assuming that  $\phi_{sat}$  and  $\phi_{orb}$  are small, so that  $R_t = -(\phi_{emf} + \phi_{to})/I_t$ . Chang *et al.* [1997] have estimated the tether resistance for the same operations presented here using the Research on Orbital Plasma Electrodynamics (ROPE) [Stone *et al.*, 1994] measurements of the satellite potential. Their results are in good agreement with tether resistances used here.

### I-V Sweeps

Many programmed sequences were developed to synchronize the operations of the individual TSS instruments. Among these, a sequence called IV24 was specifically designed to study the current-voltage response of the TSS in general, and the satellite in particular. In the deployment phase of TSS-1R the IV24 sequence was executed three times yielding, a total of 18 I-V sweeps during TSS-1R. The commanded and measured tether current and tether-Orbiter potential for a typical I-V sweep are shown in Figure 1. Note that the actual currents were less than commanded values at high current levels, resulting in significant satellite charging as the current-carrying capability of the ionosphere was tried.

The I-V data from the sweep beginning at 01:06:16 UT on February 26, 1996 are shown in Figure 2. The tether current is plotted as a function of the calculated satellite potential. Since the current is measured directly, there is little uncertainty associated with its value; less than  $\sim 0.001$ A. However, the satellite potential is determined from several measurements and has a larger uncertainty. The largest possible sources of error are the 10 V uncertainty of the Orbiter potential and the roughly 100  $\Omega$  uncertainty of the tether resistance. The error bars in Figure 2 represent an uncertainty in satellite potential of  $\pm(10+100I_t/I_o)$  volts. Also shown in Figure 2 is the curve

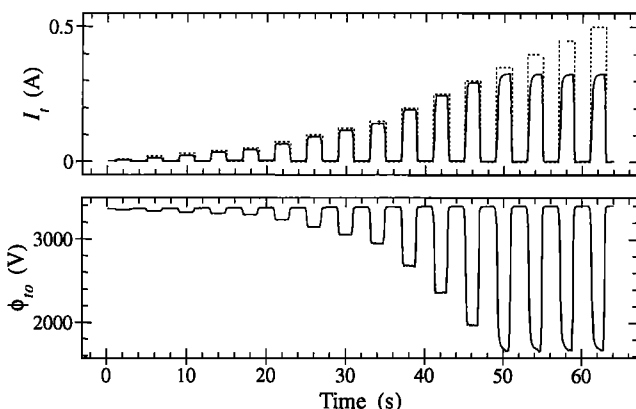


Figure 1. Commanded (dotted line) and measured (solid line) tether currents (upper panel); and measured potentials applied to EGA during a typical I-V sweep ( lower panel).

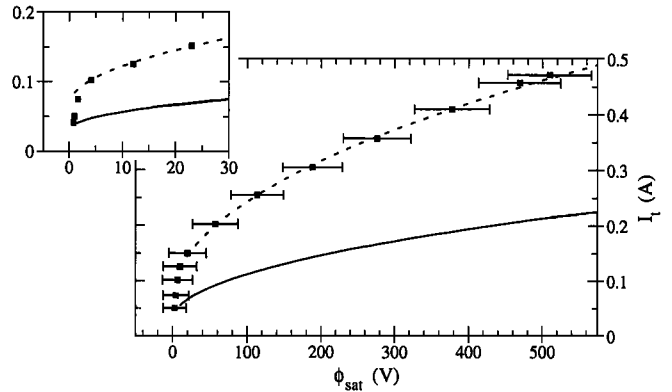


Figure 2. I-V response for a typical sweep. Data are plotted as squares with error bars representing uncertainties in the calculated satellite potential. Parker-Murphy model values are shown for this case (solid line), and multiplied by a factor of 2.17 (dotted line). The inset expands the low voltage region.

predicted by the model by Parker and Murphy [1967] which requires that the collected current be limited by the magnetic field. This model yields an I-V relationship of the form

$$\frac{I}{I_o} = 1 + \sqrt{\frac{\phi}{\phi_o}} \quad (1)$$

where  $I_o$  is the electron thermal current that would be collected by a stationary spherical probe in a magnetized plasma ( $2\pi r_{sat}^2 j_{th}$ ), and  $\phi_o$  depends on the square of the satellite radius and magnetic field,  $\phi_o = e r_{sat}^2 B^2 / 8 m_e$ . In the case shown in Figure 2,  $\phi_o$  was approximately 14 V. The magnitude predicted by the Parker-Murphy model is significantly lower than measurements during TSS-1R. However, the general shape of the I-V curve agrees well with the model above  $\sim 10$  V. This can be seen by multiplying the model result by a factor, in this case 2.17, which gives the dotted curve in Figure 2. At potentials near zero, the current is approximately  $I_o$ , but rises steeply before bending over to the square root variation. This transition region is expanded in the inset of Figure 2. In the inset, the satellite potentials are obtained from the ROPE Boom-Mounted Sensor Bias (BMSP) instrument [Stone *et al.*, 1994]. For low potentials the BMSP should provide satellite potentials subject to an uncertainty of  $\sim 1$  V, much better than the derived  $\phi_{sat}$ . The transition to square root variation is obtained by  $\sim 5$  V for this case. Interestingly, this is roughly coincident with the onset of suprathermal populations in the measured electron flux [Winningham *et al.*, 1997]. This transition to enhanced current collection is a very interesting region of the I-V characteristic seen in TSS-1R. However, more work is required obtaining accurate satellite potentials at low voltages using the satellite mounted instrumentation before quantitative results can be published.

Curves for each of the 18 I-V sweeps are shown in Figure 3, plotted as dimensionless quantities ( $I/I_o$  versus  $\phi/\phi_o$ ) in a log-log format. Note that we have limited ourselves to cases with  $\phi/\phi_o > 0.6$ . The entire data set appears in Figure 4 of Stone and Bonifazi [1997] ( $I/I_o$  versus  $\phi$ ). Also included in Figure 3 is the Parker-Murphy curve shown as a dashed line. The general agreement between the shapes of the measured and Parker-Murphy curves is evident in the log-log presentation. The measured currents are roughly 2 to 3 times larger than Parker-Murphy values over the displayed  $\phi/\phi_o$  range, with some differences between individual cases.

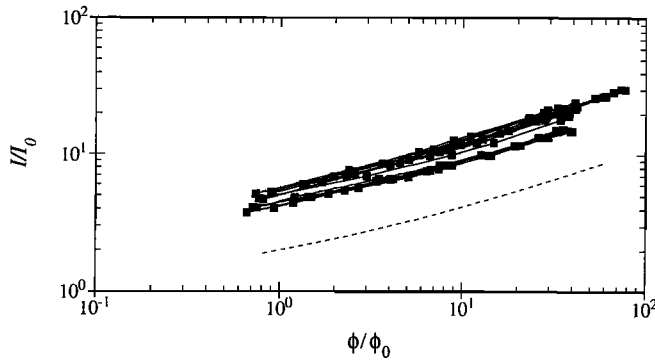


Figure 3. Plots for each of the 18 I-V sweeps (squares connected by solid lines) and the Parker-Murphy model (dashed line).

The apparent grouping of the I-V curves into two separate bands in Figure 3 cannot as yet be considered as evidence of a dependence of the current enhancement on any free parameter. The measurement uncertainties are large enough that the separation between the groups is not significant. Variations between curves appear to be within the expected measurement uncertainty.  $I_o$  varies directly with the electron density and with the square root of the electron temperature. Electron densities and temperatures, used to calculate  $I_o$ , were obtained using a satellite-mounted Langmuir probe [Dobrowolny *et al.*, 1994]. There is about 20% uncertainty in both the density and temperature measurements, which combine to give a possible error on the order of 30% for  $I_o$ . This uncertainty combined with possible errors in  $\phi_{sat}$  discussed earlier, are large enough to explain the differences between the curves. The offset of the measurements above Parker-Murphy values is large enough, however, to be significant. Work is ongoing to minimize the possible errors through careful analysis of the data. It is possible that further refinements would allow discrimination of a dependence on as yet unidentified variables.

To quantify the average I-V characteristics for TSS-1R, we have performed a best-fit analysis of each of the 18 curves

taken during the mission, fitting them to an equation of the form,

$$\frac{I}{I_o} = \alpha \left[ 1 + \left( \frac{\phi}{\phi_o} \right)^\beta \right] \quad (2)$$

The Parker-Murphy model is obtained when  $\alpha = 1$  and  $\beta = 0.5$ . Data from the 18 I-V curves are summarized in Table 1. The start time, electron density, electron temperature, maximum tether current, maximum satellite potential,  $\phi_o$ ,  $\alpha$ , and  $\beta$  are given. There was insufficient satellite charging during the three sweeps beginning at 056/23:32:50 to perform a functional fit, so  $\alpha$  and  $\beta$  are marked as N/A.  $\alpha$  is seen to range from 2.2 to 2.9, having an average of 2.5 with standard deviation of 0.30.  $\beta$  ranges from 0.47 to 0.56, averaging 0.52, with a standard deviation of 0.03.

## Discussion

The two clear results of the empirical analysis contained in the previous section are: (1) The current collected by the TSS-1R satellite varies approximately with the square root of its potential, as predicted by the Parker-Murphy model. (2) The magnitudes of the currents collected during the TSS-1R experiments were 2 to 3 times larger than predicted by this model. These conclusions are in qualitative agreement with previously reported results from the TSS-1 mission [Dobrowolny *et al.*, 1995], but extend over a substantially larger range of currents and satellite potentials. In this section we comment on consequences of the results and note some attempts to address them.

First, we note that the Parker-Murphy model has proven quite accurate for predicting both the functional shapes of I-V characteristics and the magnitudes of currents collected by sounding rockets in the ionosphere [Myers *et al.*, 1989]. The observed square root relationship suggests that like sounding rocket experiments, currents collected during TSS-1R were limited by the magnetic field in which the satellite flew. The main difference between the sounding-rocket and TSS

Table 1. Summary of the 18 I-V sweeps during TSS-1R.

GMT	$N_e$ ( $m^{-3}$ )	$T_e$ (K)	$R_t$ ( $\Omega$ )	$\phi_{sat}$ (V)	$I_t$ (A)	$\phi_o$ (V)	$\alpha$	$\beta$
056/23:20:46	$5.2 \times 10^{11}$	1400	1850	129	0.164	14.7	2.3	0.47
056/23:21:50	$5.7 \times 10^{11}$	1400	1850	104	0.166	14.1	2.2	0.47
056/23:22:54	$5.9 \times 10^{11}$	1400	1850	93	0.170	14.0	2.2	0.50
056/23:32:50	$7.0 \times 10^{11}$	1150	1850	28	0.155	14.3	N/A	N/A
056/23:33:54	$7.3 \times 10^{11}$	1150	1850	18	0.158	14.2	N/A	N/A
056/23:34:58	$8.3 \times 10^{11}$	1150	1850	16	0.163	14.6	N/A	N/A
057/00:11:58	$8.7 \times 10^{10}$	1600	1650	269	0.076	6.5	2.9	0.51
057/00:13:02	$9.8 \times 10^{10}$	1600	1650	251	0.077	6.6	2.4	0.53
057/00:14:06	$9.8 \times 10^{10}$	1600	1650	239	0.079	6.8	2.6	0.53
057/00:24:01	$9.4 \times 10^{10}$	1700	1650	229	0.083	8.5	2.9	0.55
057/00:25:05	$9.4 \times 10^{10}$	1700	1650	286	0.085	8.7	2.8	0.56
057/00:26:09	$8.4 \times 10^{10}$	1700	1650	370	0.084	9.0	2.9	0.53
057/01:06:16	$8.2 \times 10^{11}$	1400	1750	510	0.472	14.2	2.2	0.50
057/01:07:20	$8.1 \times 10^{11}$	1400	1750	567	0.466	14.2	2.3	0.49
057/01:08:24	$8.1 \times 10^{11}$	1400	1750	595	0.448	14.3	2.2	0.48
057/01:18:19	$2.7 \times 10^{11}$	1650	1750	1158	0.328	14.9	2.7	0.54
057/01:19:23	$2.8 \times 10^{11}$	1650	1750	1085	0.345	14.8	2.7	0.55
057/01:20:27	$3.2 \times 10^{11}$	1650	1750	992	0.373	14.9	2.6	0.55

experiments was the latter's supersonic speed with respect to the ionospheric ions. Models for current collection designed to explain the TSS-1R measurements must consider effects of the geomagnetic field and the high velocity of the collecting probe.

Second, since the collected current is proportional to the square root of the satellite potential, it is limited by the Earth's magnetic field. Consequently we anticipate that the flux of current-carrying ionospheric electrons to the satellite should be most intense in the directions of ram and along the magnetic field. We also anticipate that the measurements of other sensors on the satellite should provide signatures of physical processes responsible for current collection in excess of the Parker-Murphy prediction. Indeed magnetic perturbations detected during IV24 experiments show signatures of strongly anisotropic current collection [Mariani *et al.*, 1997]. It is also found that as the satellite potential exceeds the ram kinetic energy of  $O^+$  ions (5.3 eV), the level of kilohertz wave activity increases dramatically [Iess *et al.*, 1997] and a suprathermal electron population appears at the satellite's surface [Winningham *et al.*, 1997]. The distributions of wave activity and suprathermal electron fluxes are quite nonuniform around the satellite.

The challenge posed by I-V responses measured during both the TSS-1 and TSS-1R missions has elicited the development of a number of theoretical models and explanations of magnetically limited current collection by a fast moving, positively charged spacecraft in the ionosphere. Some of these investigations involve computer simulations using three-dimensional kinetic [Singh and Leung, 1997a] or fluid [Ma and Schunk, 1997] techniques. Interestingly, particle-in-cell (PIC) simulations by Singh and Leung [1997a] predict that the current to the satellite should be proportional to  $\phi_{sat}$  at low and to  $\phi_{sat}^{0.6}$  at high values. PIC simulations also predict electron heating and acceleration due to waves generated by ion reflection from the sheath potential barrier [Singh and Leung, 1997b]. More traditional analytical treatments of the interactions of electrons in the presheath [Laframboise, 1997; Cooke and Katz, 1997] and sheath [Zhang *et al.*, 1997] predict enhanced Parker-Murphy like current collection to the TSS satellite. These efforts have met with varying degrees of success in modeling the measured current enhancement. It is perhaps still too early to determine how they will contribute to a comprehensive understanding of the TSS measurements presented here.

## References

- Agüero, V., P. M. Banks, B. Gilchrist, I. Linscott, W. J. Raitt, D. Thompson, V. Tolat, A. B. White, S. Williams, and P. R. Williamson, The shuttle electrodynamic tether system on TSS-1, *Il Nuovo Cimento*, 17C, 49, 1994.
- Bonifazi, C., F. Svelto, and J. Sabbagh, TSS Core equipment, electrodynamic package and rationale for system electrodynamic analysis, *Il Nuovo Cimento*, 17C, 13, 1994.
- Burke, W. J., C. Bonifazi, D. A. Hardy, J. S. Machuzak, L. C. Gentile, D. G. Olson, C. Y. Huang, B. E. Gilchrist, J.-P. Lebreton, and C. A. Gurgiolo, Shuttle charging during EGA beam emissions of TSS 1R, *Geophys. Res. Lett.*, this issue.
- Chang, C. L., A. Drobot, D. Papadopoulos, K. H. Wright, N. H. Stone, C. Gurgiolo, J. D. Winningham, and C. Bonifazi, Temperature dependent tether resistance and its effects on the I-V characteristics of the TSS satellite, *Geophys. Res. Lett.*, this issue.
- Cooke, D. L., and I. Katz, TSS-1R electron currents: Magnetic limited collection from a heated presheath, *Geophys. Res. Lett.*, this issue 1997.
- Dobrowolny, M. and N. H. Stone, A technical overview of the TSS-1: The first Tethered-Satellite System Mission, *Il Nuovo Cimento*, 17C, 1, 1994.
- Dobrowolny, M., E. Melchioni, U. Guidoni, L. Iess, M. Maggi, R. Orfei, Y. de Conchy, C. C. Harvey, R. M. Manning, F. Wouters, J.-P. Lebreton, S. Ekholm, and A. Butler, The RETE experiment for the TSS-1 mission, *Il Nuovo Cimento*, 17C, 101, 1994.
- Dobrowolny, M., M. Guidoni, E. Melchioni, G. Vannaroni, and J.-P. Lebreton, Current voltage characteristics of the TSS 1 satellite, *J. Geophys. Res.*, 100, 23, 1995.
- Gilchrist, B. E., C. Bonifazi, S. G. Bilén, W. J. Raitt, W. J. Burke, N. H. Stone, and J. P. Lebreton, Enhanced electrodynamic tether currents due to electron emission from a neutral gas discharge: Results from the TSS-1R Mission, *Geophys. Res. Lett.*, this issue.
- Iess, L., C. Harvey, G. Vannaroni, M. Dobrowolny, J.-P. Lebreton, R. Manning, A. Onelli, and F. De Veneto, Plasma waves in the sheath of the TSS 1R satellite, *Geophys. Res. Lett.*, this issue.
- Laframboise, J. G., Current collection by a positively charged spacecraft: effects of its magnetic presheath, *J. Geophys. Res.*, 102, 2417, 1997.
- Mariani, F., M. Candidi, S. Orsini, R. Terenzi, R. Agresti, G. Musmann, M. Rahm, N. F. Ness, M. Acuna, P. Panetta, and F. Neubauer, Current flow through high-voltage sheaths observed by the TMAG experiment on TSS 1R, *Geophys. Res. Lett.*, this issue.
- Ma, T. Z., and R. W. Schunk, 3-D time-dependent simulations of the tethered satellite-ionosphere interaction, *Geophys. Res. Lett.*, this issue.
- Myers, N. B., W. J. Raitt, B. E. Gilchrist, P. M. Banks, T. Neubert, P. R. Williamson, and S. Sasaki, A comparison of current-voltage relationships of collectors in the Earth's ionosphere with and without electron beam emission, *Geophys. Res. Lett.*, 16, 365, 1989.
- Oberhardt, M. R., D. A. Hardy, W. E. Slutter, J. O. McGarity, D. J. Sperry, A. W. Everest III, A. C. Huber, J. A. Pantazis, and M. P. Gough, The Shuttle Potential and Return Electron Experiment (SPREE), *Il Nuovo Cimento*, 17C, 67, 1994.
- Parker, L. W., and B. L. Murphy, Potential buildup on an electron-emitting ionospheric satellite, *J. Geophys. Res.*, 72, 1631, 1967.
- Singh, N., and W. Leung, Three-dimensional simulation of plasma processes occurring near the tethered satellite: 1 Current collection and applicability of the Parker-Murphy model, *Geophys. Res. Lett.*, this issue.
- Singh, N., and W. C. Leung, Three-dimensional simulation of plasma processes occurring near the tethered satellite: 2. Plasma processes in the ram region, *Geophys. Res. Lett.*, this issue.
- Stenzel, R. L., and J. M. Urrutia, Transient current collection and closure for a laboratory tether, *Geophys. Res. Lett.*, this issue.
- Stone, N. H., K. H. Wright, J. D. Winningham, J. Baird, and C. Gurgiolo, A technical description of the TSS-1 ROPE investigation, *Il Nuovo Cimento*, 17C, 85, 1994.
- Stone, N. H., and C. Bonifazi, The TSS 1R mission: Overview and scientific context, *Geophys. Res. Lett.*, this issue.
- Winningham, J. D., N. H. Stone, C. A. Gurgiolo, K. H. Wright, R. A. Frahm, and C. A. Bonifazi, Suprathermal electrons observed on the TSS-1R satellite, *Geophys. Res. Lett.*, this issue.
- Zhang, T. X., K. S. Hwang, S. T. Wu, and N. H. Stone, Current collection in space using a modified Parker-Murphy model, *Geophys. Res. Lett.*, this issue.
- D. C. Thompson and W. J. Raitt, Center for Atmospheric and Space Science, Utah State University, Logan, UT 84322-4405 USA
- C. Bonifazi, Italian Space Agency, viale Regina Margherita 202, 00198, Rome, Italy
- B. E. Gilchrist, Space Physics Research Laboratory, University of Michigan, Ann Arbor, MI 48109-2143 USA
- S. D. Williams, Space Telecommunications and Radioscience Lab, Stanford University, Stanford, CA 94305-9515 USA
- J.-P. Lebreton, Space Science Department, ESA-ESTEC, 2200 AG Noordwijk, The Netherlands
- W. J. Burke, Geophysics Directorate, Phillips Laboratory, Hanscom AFB, MA USA
- N. H. Stone, Space Science Laboratory, NASA Marshall Space Flight Center, Huntsville, AL 35812
- K. H. Wright Jr., Center for Space Plasma and Aeronomic Research, University of Alabama in Huntsville, Huntsville, AL 35899

(Received January 24, 1997; revised September 22, 1997; accepted October 14, 1997)